



OPEN ACCESS

EDITED BY

Dandi Hou,
Ningbo University, China

REVIEWED BY

Xiaowen Long,
Dali University, China
Qingqing Li,
Zhongkai University of Agriculture and
Engineering, China
Leiming Wu,
Lixiahe Agricultural Institute of Jiangsu
Province, China

*CORRESPONDENCE

Qing Liu

✉ liuqing_sxau@126.com

Guojun Guo

✉ gjqzhh@hnuhae.edu.cn

†These authors contributed equally to this work

RECEIVED 23 October 2025

REVISED 29 November 2025

ACCEPTED 11 December 2025

PUBLISHED 08 January 2026

CITATION

Liu Q, He Z, Yang L, Li X, Zhai H, Zhao L, Guo G, Liu Y, Xiao L, Song J, Liu S, Wang W and Wang X (2026) Astaxanthin is not indispensable for crustaceans: carotenoid differences and metabolic mechanisms of crayfish (*Procambarus clarkii*) with different carapace colors.
Front. Mar. Sci. 12:1731102.
doi: 10.3389/fmars.2025.1731102

COPYRIGHT

© 2026 Liu, He, Yang, Li, Zhai, Zhao, Guo, Liu, Xiao, Song, Liu, Wang and Wang. This is an open-access article distributed under the terms of the [Creative Commons Attribution License \(CC BY\)](https://creativecommons.org/licenses/by/4.0/). The use, distribution or reproduction in other forums is permitted, provided the original author(s) and the copyright owner(s) are credited and that the original publication in this journal is cited, in accordance with accepted academic practice. No use, distribution or reproduction is permitted which does not comply with these terms.

Astaxanthin is not indispensable for crustaceans: carotenoid differences and metabolic mechanisms of crayfish (*Procambarus clarkii*) with different carapace colors

Qing Liu^{1,2*†}, Zhihui He^{1†}, Lirong Yang¹, Xiangyu Li¹, Huili Zhai¹, Lele Zhao¹, Guojun Guo^{3*}, Yu Liu¹, Liang Xiao⁴, Jing Song¹, Shaozhen Liu¹, Weiwei Wang¹ and Xianzong Wang¹

¹College of Animal Science, Shanxi Agricultural University, Jinzhong, Shanxi, China, ²Shanxi Agricultural University, Shanxi Key Laboratory of Animal Genetics Resource Utilization and Breeding, Jinzhong, Shanxi, China, ³College of Animal Science and Technology, Henan University of Animal Husbandry and Economy, Zhengzhou, Henan, China, ⁴Faculty of Naval Medicine, Naval Medical University, Shanghai, China

Introduction: *Procambarus clarkii* is an important economic aquatic species, and body color is an important economic trait. However, studies on the regulation of body color in crayfish remains limited.

Methods: We conducted an integrated transcriptomic and metabolomic investigation of the hepatopancreas (H) and endothelia (P) of four color variations of crayfish (N = normal, W = white, R = red-orange, and B = blue) to clarify body-color regulation mechanisms. A total of eight carotenoids were detected in the targeted metabolome; however, the types and concentrations varied considerably among the four color phenotypes or between tissues.

Results: The highest carotenoid concentrations were found in NP and NH and the lowest in WP and WH. Of the identified carotenoid types, zeaxanthin was not detected in WP. Notably, astaxanthin and canthaxanthin were found in the endothelium and hepatopancreas, whereas β -cryptoxanthin was only detected in the hepatopancreas of crayfish. For transcriptome analysis, we selected genes related to body-color regulation (crustacyanin-A2 subunit-like, crustacyanin-C1 subunit-like [*CRCN-C1*], beta,beta-carotene 15,15'-dioxygenase-like β -carotene oxygenase 1 [*BCO1*], xanthine dehydrogenase/oxidase-like [*XDH*], ABC transporter G family member 9-like [*ABCG21*], Solute Carrier Family 2 Member 3 [*SLC2A3*], and microphthalmia-associated transcription factor [*mitf*]), and analyzed the mechanism of body color formation by combining the gene expression pattern with carotenoid composition. In addition, there were four carotenoid metabolism-related pathways in the endodermis and hepatopancreas of *Procambarus clarkii* using non-targeted metabolomics techniques. In the integrated transcriptomic and metabolomic KEGG analysis,

several metabolic pathways such as vitamin digestion and absorption, retinol digestion and absorption, and purine metabolism impact the changes in differential genes such as *Sbcar1*, *NinaB*, and *XDH*, as well as differential metabolites such as xanthine, retinol, and β -carotene.

Discussion: These findings are crucial to the regulation mechanism of body color in crayfish.

KEYWORDS

body color, carotenoids, metabolomics, *Procambarus clarkii*, transcriptomics

1 Introduction

Procambarus clarkii, belonging to the subphylum Crustacea and family Decapoda, was introduced to China at the beginning of the 20th century, where it became an invasive species owing to its remarkable capacity for environmental adaptation and its disruption of natural ecosystem balance (Strychalski et al., 2022; Xiao et al., 2020). The demand for crayfish in the aquaculture market has grown recently, driven by consumer and farmer preferences, as well as the excellent fertility and nutritional value of crayfish (Ding and Kangqin, 2010). Thus, reproductive performance, nutritional value, and body color are important health indicators of crayfish. In addition, as human living standards have improved, white, red-orange, and blue crayfish have gained popularity among aquarium hobbyists for their ornamental value. Besides its economic importance, crustacean body color provides protection from environmental stressors and predators (Caro, 2005; Stuart-Fox and Moussalli, 2009).

The body color of crustaceans is regulated by endothelial pigment cells, such as erythrophores, xanthophores, and melanocytes. In particular, pigment cells are determined by the type and content of pigment granules within the cells. Carotenoids, such as astaxanthin, lutein, zeaxanthin, and carotene, are the basis of pigmentation, with astaxanthin being the most prevalent (Babin et al., 2020; Wade et al., 2017). Carotenoids cannot be synthesized by crustaceans, such as shrimps and crabs; however, they can be absorbed from their diet (Babin et al., 2019), such as from zooplankton and algae, and metabolized, transformed, or deposited directly into the epidermis or other organs via the hepatopancreas. The metabolic conversion pathways of carotenoids in shrimp, lobsters, and crabs are notably similar to that of β -carotene to astaxanthin via echinenone, canthaxanthin, and zeaxanthin (Jiao et al., 2023; Simpson and Chichester, 1976). However, a second metabolic pathway also exists in shrimp: the metabolism of zeaxanthin to astaxanthin as a substrate (Shimaya et al., 1972). For instance, *Tigriopus californicus*, an associated crustacean, utilizes β -carotene as a metabolic substrate in three different metabolic pathways that result in the formation of astaxanthin via hydroxylation and ketone acylation (Weaver et al., 2018). Therefore, it appears that supplementing crustacean

diets with carotenoids could be an effective way to enhance their pigmentation and overall economic and aesthetic value. It is amazing how much impact small changes such as this can have on the market and consumer perception.

The *CRCN* gene was found in crustaceans, such as the prawns (*Macrobrachium rosenbergii*) (Wang, 2012) and European lobsters (*Homarus gammarus*) (Cianci et al., 2002), which regulates the combination of astaxanthin with sterols to form chromophores, influencing body-color variations. For instance, high astaxanthin content, coupled with certain proteins, enhances the green color of river crab carapaces. During high-temperature cooking, as the carotenoid-protein complex denatures and inactivates, the hydrogen bond between the carotenoids and proteins breaks, detaching from proteins and turning the carapace to a reddish-orange color. Esterified astaxanthin and free astaxanthin are interconverted, and different environmental background colors can change the color of crustaceans; however, the total astaxanthin content remains constant in the body (Wade et al., 2012).

In addition to carotenoids, crustaceans possess pteridine pigments that contribute to their red and yellow body coloration; these pigments have been extensively studied in teleost fish (Kimura, 2021; Oliphant and Hudon, 1993). Moreover, melanosomes are present in melanocytes, carotenoid vesicles, and red- or yellow-pigment vesicles with purine or pyrimidine, which are major components of xanthophores and erythrophores (Ichikawa et al., 1998; Saunders et al., 2019; Volkening and Sandstede, 2018). Of these, pteridine—comprising a heterocyclic complex of pyrimidine and pyrazine rings—is widely found in insects. Pteridine pigments synthesize tetrahydrofolate from guanosine triphosphate (GTP), which is then converted to tetrahydrobiopterin (BH4), an essential cofactor in the melanin synthesis pathway (Hu et al., 2020). In a previous study, BH4 deficiency in the silkworm affected pteridine synthesis and melanin substance production (Bonafé et al., 2001; Wijnen et al., 2007).

Comparative transcriptome and metabolomics based on trait mutations are important means of studying the formation mechanisms of excellent traits and the evaluation of genetic resources in animals. Albino is a common phenotype of crustaceans. White crayfish with a recessive inheritance mode

were discovered in natural waters in 1999 (Nakatani, 1999). Studies on body color in *Drosophila* and houseworms have revealed that mutations in the *white* gene create the albino phenotype (Liu et al., 2013, 2011). However, the body-color mutation of crayfish has many types. Not only is the whitening mechanism unclear, but the process of body-color change is also rarely known. To address these issues, it is necessary to clarify the unique body-coloration mechanism of crayfish. In this study, we focused on the three body-color mutants of crayfish and used multiomics methods such as combined comparative transcriptome, carotenoid-targeted metabolome, and nontargeted metabolome analysis to determine the regulation process of differential genes and differential metabolites in the body-color variation-related pathways of crayfish and the molecular mechanism of body-color formation. This study not only helps in the understanding of the carotenoid metabolism process of crustaceans but also provides basic genetic information for crustacean body-color breeding.

The rapid expansion of crayfish aquaculture, particularly of *Procambarus clarkii*, raises significant concerns regarding ecological safety and the broader One Health framework, which emphasizes the interconnectedness of human, animal, and environmental health. As an invasive species, *P. clarkii* poses a threat to native biodiversity through competition, predation, and habitat modification, particularly in wetland ecosystems (Xiao et al., 2020). Unregulated farming and accidental release into natural waterways can exacerbate these impacts, leading to long-term ecological imbalances. Furthermore, intensive aquaculture practices may contribute to water pollution, antibiotic resistance, and disease transmission between wild and farmed populations. From a One Health perspective, ensuring sustainable crayfish farming requires integrated management strategies that

include biosecurity measures, environmental monitoring, and responsible breeding practices. Understanding the genetic and metabolic basis of traits such as body color not only supports selective breeding for desirable phenotypes but also enables the development of strains with reduced environmental impact. For example, genetically stable, non-invasive color variants could be promoted in ornamental aquaculture to minimize the risk of ecological escape and establishment. Thus, integrating multiomics research with ecological risk assessment and public health considerations is essential for advancing sustainable and safe aquaculture systems under the One Health paradigm.

2 Materials and methods

2.1 Ethics approval and consent to participate

The experimental animal treatments in this study were consistent with animal protection, animal welfare and ethical principles, and in accordance with the relevant provisions of the national experimental animal ethical welfare and approved by the Institutional Animal Care and Use Committee of Shanxi Agricultural University.

2.2 Sample collection

A total of 36 normal crayfish (N), white crayfish (W), red-orange crayfish (R), and blue crayfish (B) were bred and cultured in our

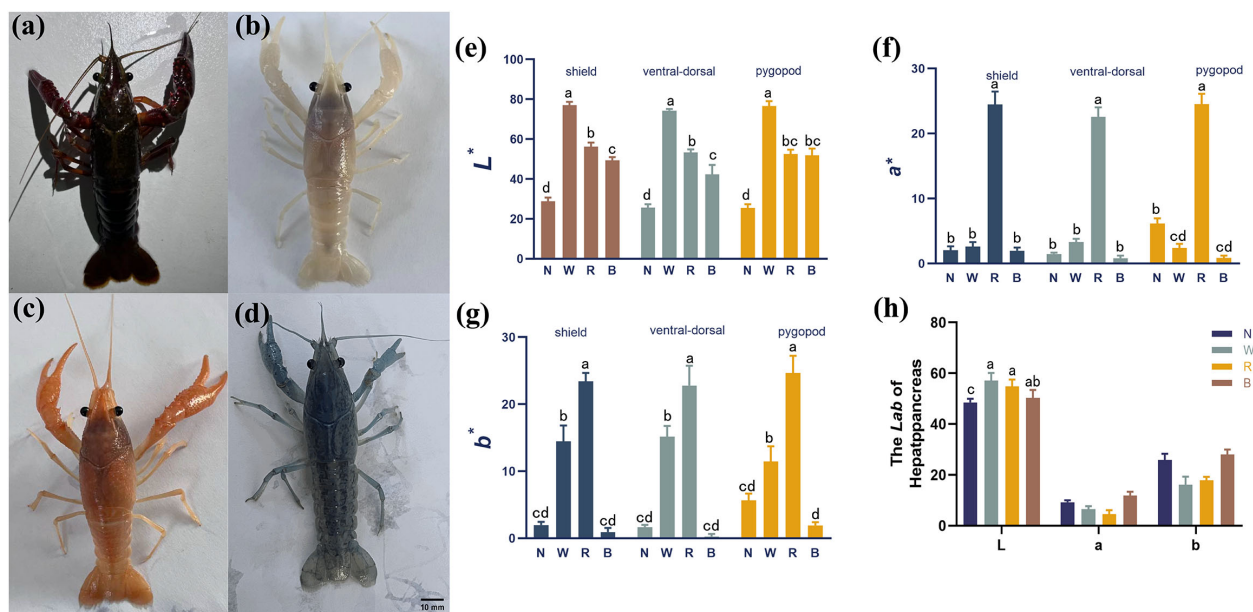


FIGURE 1

Four body-color variations of crayfish used in this study (a–d) and their histogram of endothelial (including shield, ventral-dorsal, and pygopod measurements) and hepatopancreatic lab values (e–h). (a) Normal (N), (b) white (W), (c) red-orange (R), (d) blue (B), (e) lab values for L*, (f) lab values for a*, (g) lab values for b*, (h) lab values of hepatopancreatic for L*, a*, and b* (a–d indicated that the difference of L*, A* and B* in the same part was significant, P < 0.05).

laboratory (Figures 1a–e). The shrimp and crab were fed twice a day (9:00 and 18:00); the total daily feed amount was 5% of their body weight, with 30% provided in the morning and 70% in the afternoon. The feed residues and excreta were cleaned before each feeding. Nine crayfish from each of the four body-color groups were randomly selected (three replicates of each body color) after a growth period of 1 year for analysis (average adult weight: 26.6 ± 6.3 g). Culture water was continuously aerated (24 h) at a temperature of 20–23°C, pH 7.9, salinity 5.3 ‰, ammonia–nitrogen 0.2 mg L^{-1} , nitrite $0.005\text{--}0.01 \text{ mg L}^{-1}$, and dissolved oxygen $6.0\text{--}10.0 \text{ mg L}^{-1}$. The photoperiod was 12 h light / 12 h dark, with a light intensity of 500–600 lx. The crayfish were anesthetized on ice for 40 seconds before sample collection. The hepatopancreases and endocarps of each crayfish were removed using scissors and forceps, immediately frozen in liquid nitrogen and stored in a -80°C refrigerator until further analysis.

2.3 Phenotypic measurements and pigment cell observations

Corresponding color parameters and carotenoids were measured in portions of the endocarps and hepatopancreases from each crayfish species. Body-color measurements on the shield, ventral-dorsa, and pygopod of each crayfish carapace were taken using a precision colorimeter (3nh, NR110, China). The International Commission on Illumination (CIE) uniform chromaticity spatial system CIE $L^*a^*b^*$ (CIE1931) was adopted, accounting for parameters such as the determination of luminance (L^*), redness (a^*), and yellowness (b^*). The endocarps and hepatopancreases were harvested from each crayfish for to determine of carotenoids after body-color measurements were taken. Carotenoid values were measured, and pigment cell types, morphologies, and sizes were observed under a continuous-magnification stereomicroscope (Cnoptec, SZ680, China) (2.0×).

2.4 RNA extraction, library construction, and sequencing

Endothelial and hepatopancreatic total RNA was extracted using a Trizol kit (Invitrogen), following to the manufacturer's instructions. RNA quality was assessed using an Agilent 2100 Bioanalyzer (Agilent Technologies, Palo Alto, CA, USA) and verified using RNase-free agarose gel electrophoresis. After extracting total RNA eukaryotic mRNA was enriched using Oligo (dT) beads. The library was constructed using the NEBNext Ultra RNA Library Prep Kit for Illumina (NEB #7530, New England Biolabs, Ipswich, MA, USA). The purified double-stranded cDNA fragments were end repaired; subsequently a base was added and ligated to Illumina sequencing adapters. The ligation reaction was purified using AMPure XP Beads (1.0X). Meanwhile, polymerase chain reaction (PCR) was used to amplify target gene sequences. The resulting cDNA library was sequenced using Illumina Novaseq6000 by Gene Denovo Biotechnology Co. (Guangzhou, China).

2.5 Differentially expressed gene analysis

Reads obtained from the sequencing machines included raw reads containing adapters or low-quality bases, which could negatively impact the assembly and analysis. Thus, to obtain high-quality clean reads, the raw reads were further filtered using fastp software (version 0.18.0) (Chen et al., 2018). An index of the reference genome was established, and paired-end clean reads were mapped to the reference genome using HISAT2 (version 2.4) with default parameter settings (Kim et al., 2015). Subsequently, the read alignments were sorted using Samtools (version 1.17) (Danecek et al., 2021), and transcripts were reconstructed using genome-guided *de novo* assembly approaches using Trinity (version 2.12.0) (Haas et al., 2013). Principal component analysis (PCA) was performed using the gmodels package (<http://www.r-project.org/>) for R (v2.18.1). RNA differential expression analysis between the two groups was conducted using DESeq2 software (Love et al., 2014). Genes with a false discovery rate (FDR) of < 0.05 and absolute fold change (FC) of ≥ 2 were considered differentially expressed. The genes were annotated using the KEGG ontology database. Meanwhile, functional annotation and pathway enrichment analyses were performed for DEGs using KEGG gene IDs (Wu et al., 2021).

2.6 Metabolite extraction and LC-MS/MS analysis

Harvested endothelia and hepatopancreas were quickly frozen in liquid nitrogen after dissection. Tissues (~80 mg) were cut on dry ice and placed in an Eppendorf tubes (2 mL). Subsequently, tissue samples were then homogenized with 200 μL of H_2O and five ceramic beads using the homogenizer (MP, FastPrep-24 5G). Afterward, 800 μL of methanol/acetonitrile (1:1, v/v) was added to the homogenized solution for metabolite extraction, after which the mixture was centrifuged for 15 min ($14,000\times g$, 4°C). The supernatant was dried in a vacuum centrifuge. For LC-MS analysis, the samples were redissolved in 100 μL acetonitrile/water (1:1, v/v) solvent. Quality control samples were prepared by pooling 10 μL of each sample to monitor the stability and repeatability of the instrument analysis, which were analyzed alongside the other samples.

For HILIC separation, samples were analyzed using a 2.1 mm \times 100 mm ACQUITY UPLC BEH 1.7 μm column (Waters, Ireland). In ESI-positive and ESI-negative modes, the mobile phase contained A = 25 mM ammonium acetate and 25 mM ammonium hydroxide in water and B = acetonitrile. The gradient was 85% B for 1 min, linearly reduced to 65% in 11 min, then 40% in 0.1 min and kept for 4 min, and then increased to 85% in 0.1 min, with a 5-min re-equilibration period.

An AB TripleTOF 6600 mass spectrometer was used for the analysis. The ESI source conditions after HILIC chromatographic separation were as follows: in ESI-positive and ESI-negative modes, ion source gas 1 (60), ion source gas 2 (60), and curtain gas. The secondary mass spectrum was obtained via information-dependent acquisition (IDA) using the high-sensitivity mode. In ESI-positive

and ESI-negative modes, the declustering potential is ± 60 V, collision energy is 35 ± 15 eV, and IDA was set as follows: excluding intrusion within 4 Da and 10 candidate ions to monitor per cycle.

2.7 Metabolomics-bioinformatics analysis

The raw MS data were converted to mzXML files using ProteoWizard MSConvert before importing into freely available XCMS software. Orthogonal partial least squares discriminant analysis (OPLS-DA) was conducted using the packages gmodels and ropls (R v2.18.1) (Warnes et al., 2018). Subsequently, we combined the variable importance in projection (VIP) value of the OPLS-DA and the P value of the univariate statistical analysis t -test to screen for differential metabolites between the comparison groups (Saccenti et al., 2014). The threshold value of the difference was $VIP \geq 1$, and significance threshold was $P < 0.05$.

For KEGG annotation and enrichment analyses, the identified metabolites were annotated using the KEGG compound database (<http://www.kegg.jp/kegg/compound/>). Subsequently, the annotated metabolites were mapped to the KEGG Pathway database (<http://www.kegg.jp/kegg/pathway.html>). Pathways with differential metabolites were fed into metabolite sets for enrichment analysis, and the significance of such enrichment was determined by the resulting P value.

2.8 Integrative analysis of metabolome and transcriptome

For the joint analysis of the histology, we took the mean values of the six sets of samples in the metabolic group two by two to correspond with the transcriptome data. Two-way orthogonal partial least squares (O2PLS) analysis was conducted using the OmicShare online tool (<https://www.omicshare.com/tools/>). Differentially expressed genes ($FDR < 0.05$ and $|\log_2FC| > 1$) and differential metabolites ($VIP > 1$ and $P < 0.05$) were analyzed in the following pairwise groups: NP vs. WP, NP vs. RP, NP vs. BP, and NH vs. WH, NH vs. RH, and NH vs. BH. O2PLS was conducted using the integral quantitative values of DEGs and differential metabolites from transcriptome analysis to screen for associated genes and metabolites.

2.9 Targeted carotenoids omics analysis

Three crayfish from the same tank were set up as one biological replicate for a total of three biological replicates for the three tanks. The samples used for targeted carotenoid omics analysis were the same as that for the not-target analysis. Approximately 1 mL of methanol and 0.1% BHT were added to the accurately weighed endocarps and hepatopancreases (0.1–0.5 g). Subsequently, the sample was homogenized and left to stand overnight at 4°C. The next day, the samples were centrifuged at 3000 rpm for 5 min. The

methanol layer was transferred into a 2mL volumetric flask. Afterward, 1mL of n-hexane was added to the remaining sample in the vial, vortexed for 30 s, and then centrifuged at 3000 rpm for 5 min. The n-hexane layer was transferred into a fresh test tube. This procedure was repeated one more time using 1mL n-hexane, followed by evaporation to dryness under a gentle flow of nitrogen at 30°C. The residue was reconstituted with 0.2 mL methanolic solution.

The sample extracts were analyzed at 450 nm using a UPLC system equipped with a DAD detector (UPLC, U3000; Thermo). The analytical conditions were as follows: UPLC column; YMC Carotenoid S-3um (150 mm×4.6 mm); column temperature, 40°C; flow rate, 1.0 mL/min; injection volume, 2 μ L; solvent system, MeOH (MeOH:MTBE:H₂O=20: 75: 5); and gradient program, 100:0 V/V at 0 min, 39:61 V/V at 15 min, 0:100 V/V at 25 min, 100:0 V/V at 25.1 min, and 100:0 V/V at 30 min. Concentrations of 0.1–17.5 μ g/mL of standard samples with astaxanthin, lutein, zeaxanthin, β -cryptoxanthin, α -carotene, β -carotene, neoxanthin, violaxanthin, capsanthin, xanthophyll, and lycopene were used in the analysis.

2.10 Analysis of body color related gene expression patterns

Genes related to body color were selected from endothelial and hepatopancreatic transcriptome analyses for quantitative real-time PCR (qRT-PCR), to investigate the body color regulatory mechanisms of crayfish. Targeted carotenoid-related genes were *CRA2*, *CRC1*, and *BCO1*; melanin-related genes were *SLC2A3* and *mitf*; and pteridine-related genes were *ABCG21* and *XDH*. Total RNA extracted from endothelia and hepatopancreas (1 μ g) was reverse transcribed into cDNA. The system was supplemented to 10 μ L with 1 μ g of RNA, 2 μ L of 5 \times gDNA eraser buffer, 1 μ L of gDNA eraser, and RNase-free dH₂O. Subsequently, the solution was incubated at 42°C for 2 min. Afterward, 1 μ L of PrimeScript RT Enzyme Mix I, 1 μ L of RT Primer Mix, 4 μ L of 5 \times PrimeScript Buffer 2, and 4 μ L of RNase-free dH₂O were added to the reaction solution on ice. The mixture was reacted at 37°C for 15 min, and then again at 85°C for 5 s. Primer Premier 5.0 software was used to design qRT-PCR primers using 18s rRNA as the internal reference gene (Yu et al., 2022). Supplementary Table 1 presents primer amplification sizes. Subsequently, 10 μ L of total qRT-PCR mix, comprising 1 μ L cDNA template, 5 mL 2 \times Universal SYBR Green qPCR Supermix, 0.5 μ L upstream and downstream primers, and 3 μ L ddH₂O, was used for qRT-PCR, which was conducted on a QuantStudio 6 Real-Time PCR system (Applied Biosystems, USA). Data were statistically analyzed using the $2^{-\Delta\Delta Ct}$ method.

3 Results

3.1 Differences in body color among the four body-color variations of crayfish

We analyzed the color parameters of the carapaces and hepatopancreases of crayfish to identify notable differences in

color among the four body colors. The crayfish shield, ventral-dorsal, and pygopod of the three parts of the carapaces and hepatopancreases were positive in all four body colors, as shown in Figures 1a–h. In particular, the L^* values of the hepatopancreases and carapaces exhibited a consistency pattern ($N < B < R < W$, Figures 1e, h); however, the a^* and b^* of the carapaces were different, following the order of $B < N < W < R$ (Figures 1f, g). The consistency pattern of the hepatopancreas a^* and b^* values was opposite ($R < W < N < B$, Figure 1h) to that of the carapace values. The carapace L^* of the white crayfish was significantly higher ($P < 0.05$) than those of the other three crayfish, and the carapace L^* of the normal crayfish was significantly lower ($P < 0.05$) than those of the other three crayfish (Figure 1e). In addition, the carapace a^* and b^* values of red–orange crayfish were significantly higher ($P < 0.05$) than those of normal, white, and blue crayfish (Figures 1f, g).

3.2 Pigment cell observation

Stereomicroscope observations indicated that the crayfish carapace had four body colors resulting from xanthophores, erythrophores, and blue pigment cells. The normal body color of crayfish carapaces is dominated by erythrophores, where pigment cells are widely dispersed and dark red, mostly with punctate and dendritic distribution (Supplementary Figure A). In the carapaces of white crayfish, only xanthophores were found, and they were primarily scattered in dots with a less dense, yellowish tint (Supplementary Figure B). The carapace of red–orange crayfish primarily comprised erythrophores; however, there were also a few visible xanthophores, which were dense, less cellular, and mostly found as extended dendrites (Supplementary Figure C). Erythrophores and blue pigment cells predominated in the carapaces of blue crayfish and they were more densely distributed than the blue pigment cells. However, their density was still smaller than that in normal crayfish coloration, and they were primarily distributed as dots. Moreover, the carapace in blue crayfish contained a mixture of dark red erythrophores and blue pigment cells (Supplementary Figure D).

3.3 Carotenoid type and content analysis

We investigated the carotenoid concentrations in the endodermises and hepatopancreases of the four color variations of crayfish species to explore carotenoid variations across and between tissues. By measuring the target metabolites, the astaxanthin, neoxanthin, violaxanthin, lutein, zeaxanthin, β -cryptoxanthin, carotene and β -carotene levels were established (Supplementary Table 2). The findings indicate that astaxanthin existed in the hepatopancreases and endodermis of white, red–orange, and blue crayfish although the absolute values of the content significantly differed. The hepatopancreases and endodermis of the normal crayfish had the highest absolute values and the greatest number of the seven carotenoid types.

There were only three types of carotenoids found in the endodermises and hepatopancreases of white crayfish: lutein, β -carotene, and astaxanthin. In addition, the absolute values of the content were the lowest in white crayfish. β -cryptoxanthin was not detected in the endothelium of any crayfish, regardless of body color. Instead, β -cryptoxanthin was found to be specific to the hepatopancreas and was not detected in the WH group. Moreover, zeaxanthin was also not detected in the white crayfish endodermis. The carotenoid content in the hepatopancreas of the normal crayfish was 2 to 12 times higher than that of the other color variations. A comparison of the total carotenoid content of the endodermises of the four body colors of crayfish resulted in a consistency pattern of $NP > RP > BP > WP$. $BH > NH > RH > WH$ was the order of total carotenoid concentration in the hepatopancreatic samples, because blue crayfish hepatopancreases had the highest amount of β -carotene (35.3322 $\mu\text{g/mL}$). The four color variations of crayfish clearly differ according to carotenoid species and content, which regulate variances in body color. Within the metabolic pathway of secondary metabolites, we identified three carotenoid-related metabolites (β -cryptoxanthin, fucoxanthin, and zeaxanthin) and two differential metabolites (astaxanthin and canthaxanthin) in the endothelia, however, only astaxanthin and canthaxanthin were found in the hepatopancreas.

3.4 Differentially expressed genes in the endothelia and hepatopancreas in four body-color variations of crayfish

To explore the differences in gene expression among the four body colors of crayfish, RNA-seq was conducted in three replicates. Q30 and Q20 were $>92\%$ and $>97\%$ for every group in the endothelium and hepatopancreas, respectively, indicating that all of the sequencing data could be further analyzed (Table 1). In PCA, the FPKM value for each gene was determined. In biological duplicates, the PCA distribution structure indicated comparable expression patterns (Figures 2i, j).

The distribution of fold change and the P value of the genes were determined to validate the differentially expressed genes ($FC \geq 2$; P value < 0.05), as shown in Figures 2a–f. In the endothelial samples, a total of 828 differentially expressed genes were found between NP and WP: 513 and 315 upregulated and downregulated genes, respectively. Moreover, there were 951 differentially expressed genes between NP and RP: 698 and 253 upregulated and downregulated genes. A total of 4,402 differentially expressed genes were measured in NP vs. BP: with 1,303 and 3,099 upregulated and downregulated genes, respectively (Figure 2g). Hepatopancreatic samples revealed 2,972 differentially expressed genes in NH vs. WH (1698 and 1274 downregulated and upregulated, respectively), 2270 differentially expressed genes between NH and RH (1285 and 985 downregulated and upregulated, respectively), 4768 differentially expressed genes between NH and BH (3006 and 1762 downregulated and upregulated, respectively) (Figure 2h).

TABLE 1 Transcriptome sequencing data of the endothelium and hepatopancreas.

Sample	RawReads/bp	CleanReads/bp	Q20	Q30%	Gene_num
NP1	37935910	37795304	97.90	94.04	13135
NP2	38858502	38705840	97.90	94.13	13796
NP3	43014546	42856212	97.79	93.83	13299
WP1	41907846	41770358	97.50	92.92	14016
WP2	36188434	36041710	97.93	94.07	14005
WP3	40197100	40050958	97.99	94.24	12840
RP1	36970462	36825942	97.52	93.13	13265
RP2	37112574	36968226	98.00	94.38	13392
RP3	39566072	39227198	97.32	93.12	14811
BP1	40665364	40510474	97.85	93.80	10563
BP2	39720776	39566844	98.03	94.43	11440
BP3	43696000	43541260	97.83	93.81	11126
NH1	45052704	44888180	97.96	94.19	13736
NH2	48742000	48516038	97.53	93.26	13516
NH3	40565664	40405896	97.77	93.82	13673
WH1	40029062	39874038	97.96	94.21	13491
WH2	42041646	41888404	98.00	94.36	13609
WH3	40221666	40077600	98.06	94.51	13336
RH1	38287044	38112960	97.49	93.19	12982
RH2	41821794	41666976	97.76	93.79	13510
RH3	36102878	35957552	97.72	93.57	12975
BH1	42946808	42758224	97.81	93.92	11990
BH2	43504124	43354746	97.96	94.24	11013
BH3	42930958	42759540	97.72	93.76	11908

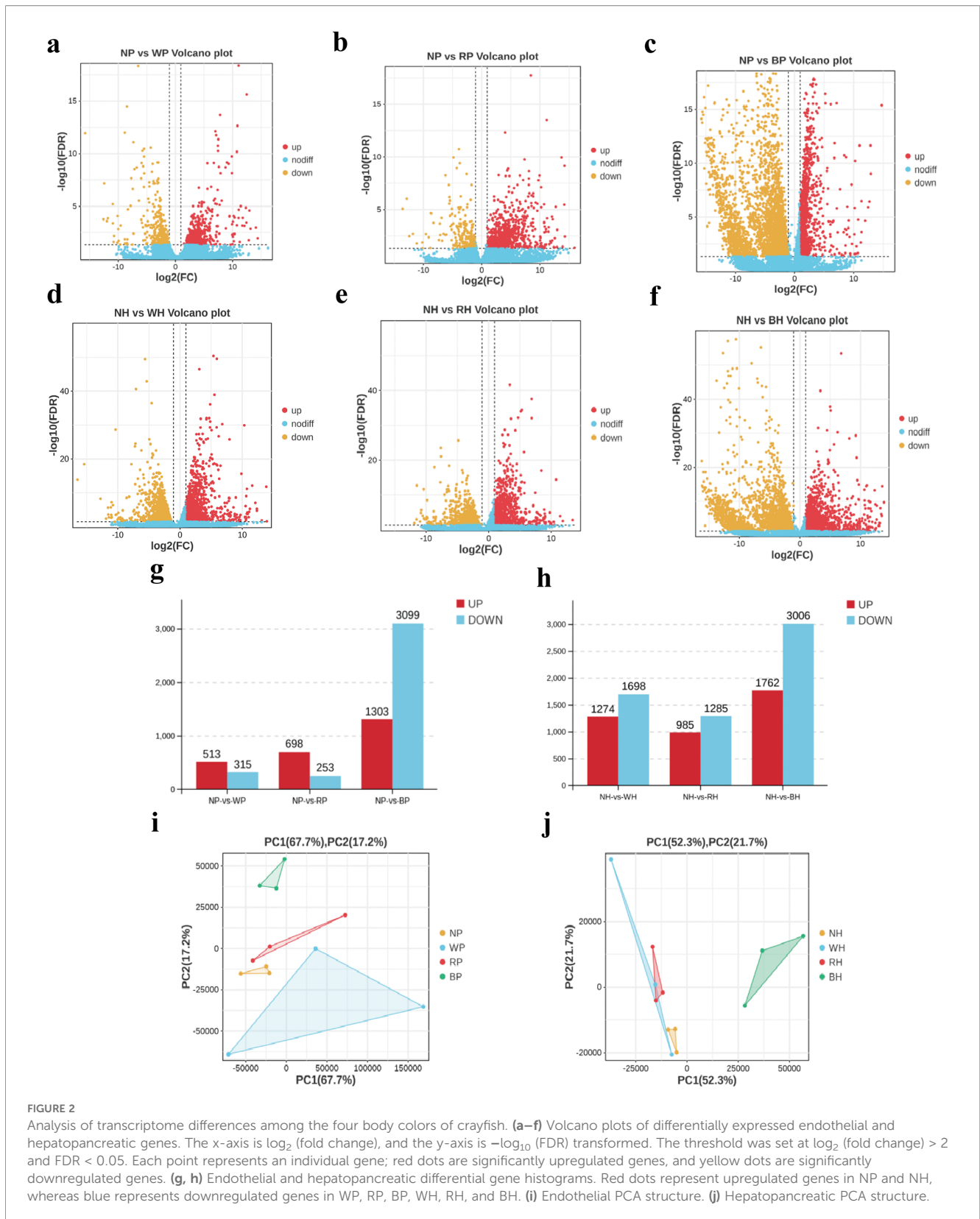
3.5 KEGG enrichment analysis of differentially expressed genes

We conducted KEGG annotation analysis of differentially expressed genes to further explore the biological functions of differentially expressed genes. The differentially expressed genes in the endothelium and hepatopancreas of four body colors of crayfish were annotated into six KEGG databases: metabolic processes, human diseases, organismal systems, cellular processes, genetic information processes, and environmental information processes. Differentially expressed genes were enriched in 294, 291, and 345 KEGG pathways in the NP and WP, NP and RP, as well as NP and BP groups, respectively. The pathways of the top 10 were selected for display based on the *P* value (Supplementary Table 3). The results indicate that the differentially expressed genes in the NP and WP groups were significantly enriched in the pathways of metabolic, pantothenate and CoA biosynthesis, and the IL-17 signaling pathway. Differentially expressed genes in the NP and RP groups were significantly enriched in pathways such as

amebiasis, renin-angiotensin system, and phenylalanine metabolism. Meanwhile, differentially expressed genes in the NP and BP groups were in metabolic pathways such as cardiac muscle contraction, ribosome biogenesis in eukaryotes, and hypertrophic cardiomyopathy. Differentially expressed genes were involved in 344, 341, and 348 KEGG pathway enrichments in the NH/WH, NH/RH, and NH/BH groups, respectively. Differential genes were significantly enriched in metabolic pathways such as endocytosis, metabolic pathways, pentose and glucuronate interconversions, and other metabolic pathways in NH and WH, coronavirus disease-COVID-19, ribosome, metabolic pathways, and other pathways.

3.6 Expression of body color-related genes

We selected genes related to body color, including *CRA2*, *CRC1*, *BCO1*, *ABCG21*, *XDH*, *SLC2A3*, and *mitf*, in our transcriptomics analyses to further investigate the metabolism of body color-related



pigments in the four body colors of crayfish. Among the four body colors, NP and NH exhibited high expression of *CRA2* and *CRC1*, (Figures 3b, i) whereas WP, RP, BP, WH, RH, and BH exhibited low or no expression (Figures 3a, h). Moreover, *BCO1* expression was

higher in the endothelia than in the hepatopancreases in the crayfish, regardless of body color. *BCO1* expression was low in NP but high in BP and BH, and expression in NH was significantly higher than that in WH compared with RH (Figures 3c, j). In WP,

ABCG21 and *XDH* exhibited high expression levels; however, in NP, their expression levels were significantly low, and in RP and BP, expression levels were either nonexistent or significantly low. In RH, *ABCG21* and *XDH* were substantially expressed; in NH, *XDH* was less expressed than in WH; and *ABCG21* was more expressed than in WH, whereas neither gene was expressed in BH (Figures 3d, e, k, l). The expression levels of the melanin-related genes *SLC2A3* and *mitf* were high in WP, low in NP and RP, and not present in BP. In WH, RH, and NH, *SLC2A3* and *mitf* were expressed; however, in BH, they were either nonexistent or significantly low. *SLC2A3* expression was higher in WH than in NH, RH, and BH, and *mitf* was expressed higher in NH than in WH and RH (Figures 3f, g, m, n).

3.7 Differential metabolites in the endothelium and hepatopancreas of the four body colors of crayfish

Six biological replicates for each of the four body colors of crayfish were used for the metabolic analyses of the endothelia and hepatopancreas (each biological replicate contained three individuals). There were 11,611 and 12,218 metabolites in total in the POS and NEG modes, respectively, across the endothelial samples. Meanwhile, 12,395 and 11,202 metabolites in total in the POS and NEG modes were identified in the hepatopancreatic samples (Table 2).

OPLS-DA VIP values and t-test *P* values ($VIP \geq 1$, $P < 0.05$) were used to evaluate metabolites that exhibited significant differences between groups. The differential metabolites from the NEG and POS models were integrated and analyzed. Six comparison groups were created from the endothelia and hepatopancreas of crayfish with four different body colors (NP vs. WP, NP vs. RP, and NP vs. BP as well as NH vs. WH, NH vs. RH, and NH vs. BH; Figures 4h, g). In the endothelial samples (Figures 4a–c), there were 441 differential metabolites in NP vs. BP (346 and 95 upregulated and down-regulated metabolites, respectively), 370 differential metabolites in NP vs. RP (120 and 250 upregulated and downregulated metabolites, respectively), and 367 differential metabolites in NP vs. WP, (162 and 205 upregulated and downregulated metabolites, respectively). In hepatopancreatic samples (Figures 4d–f), 455 upregulated and 93 downregulated metabolites were identified in 548 differential metabolites in NH vs. WH; 454 upregulated and 118 downregulated metabolites were obtained in 572 differential metabolites in NH vs. RH; and 315 upregulated and 189 downregulated metabolites were identified in 504 differential metabolites in NH vs. BH (Figures 4d–f).

3.8 KEGG enrichment analysis of differentially abundant metabolites

We annotated differential metabolites in KEGG databases for analysis to further explore the role of differential metabolites in metabolic pathways. A total of seven categories of KEGG databases

were annotated for differential metabolites in the endothelium and hepatopancreas of the four body colors crayfish: metabolic processes, organismal systems, human diseases, drug processes, environmentally informative processes, genetically informative processes, and cellular processes. Differential metabolites were involved in the metabolic processes of 129, 97, and 128 KEGG pathways in the NP vs. WP, NP vs. RP and NP vs. BP groups, respectively. The top 10 pathways were selected for display based on the *P* value (Supplementary Table 4). The results indicate that differential metabolites were significantly enriched in metabolic pathways such as vitamin B6 metabolism, histidine metabolism, ubiquinone and other terpenoid–quinone biosynthesis. In the NP and RP groups, differential metabolites were significantly enriched in ubiquinone and other terpenoid–quinone biosynthesis and other metabolic pathways. Differential metabolites in the NP and RP groups were significantly enriched in ubiquinone and other terpenoid–quinone biosyntheses, steroid hormone biosynthesis, steroid hormone biosynthesis, and prostate cancer. Differential metabolism was significantly enriched in the NP and BP groups for insulin resistance, sphingolipid signaling pathway, metabolic pathways, and other pathways. sphingolipid signaling pathway, metabolic pathways and other pathways. Differential metabolites were enriched in 110, 163, and 136 KEGG-enrichment pathways in the NH vs. WH, NH vs. RH, and NH vs. BH groups, respectively. Differential metabolites in the NH and WH groups were enriched in enrichment pathways such as tryptophan metabolism, phenylalanine, tyrosine and tryptophan biosynthesis, and metabolic pathways. Differential metabolites in the NH and RH groups were enriched in metabolic pathways such as metabolic pathways, pyrimidine metabolism and ABC transporters. Differential metabolites in the NH and BH groups were enriched in the metabolism of taurine and hypotaurine metabolism, neuroactive ligand–receptor interaction, and pentose and glucuronate interconversion. Differential metabolites in the NH and BH groups were enriched in metabolic pathways such as taurine and hypotaurine, metabolism, neuroactive ligand–receptor interaction, pentose and glucuronate interconversion, and other enrichment pathways.

3.9 Differentially expressed gene and differential metabolite KEGG enrichment analysis

KEGG enrichment analysis of differentially expressed endothelial and hepatopancreatic genes with differential metabolites revealed that the NP vs. WP, NP vs. RP, and NP vs. BP groups were enriched in 99, 73, and 110 pathways, respectively. Similarly, the NH vs. WH, NH vs. RH, and NH vs. BH groups were enriched in 94, 101, and 114 pathways, respectively. Among the pathways associated with body color were vitamin digestion and absorption, ABC transporters, glycolysis and gluconeogenesis, arachidonic acid metabolism, melanogenesis, and purine metabolism. There were a total of 131 differentially expressed genes and 50 differentially expressed metabolites in the

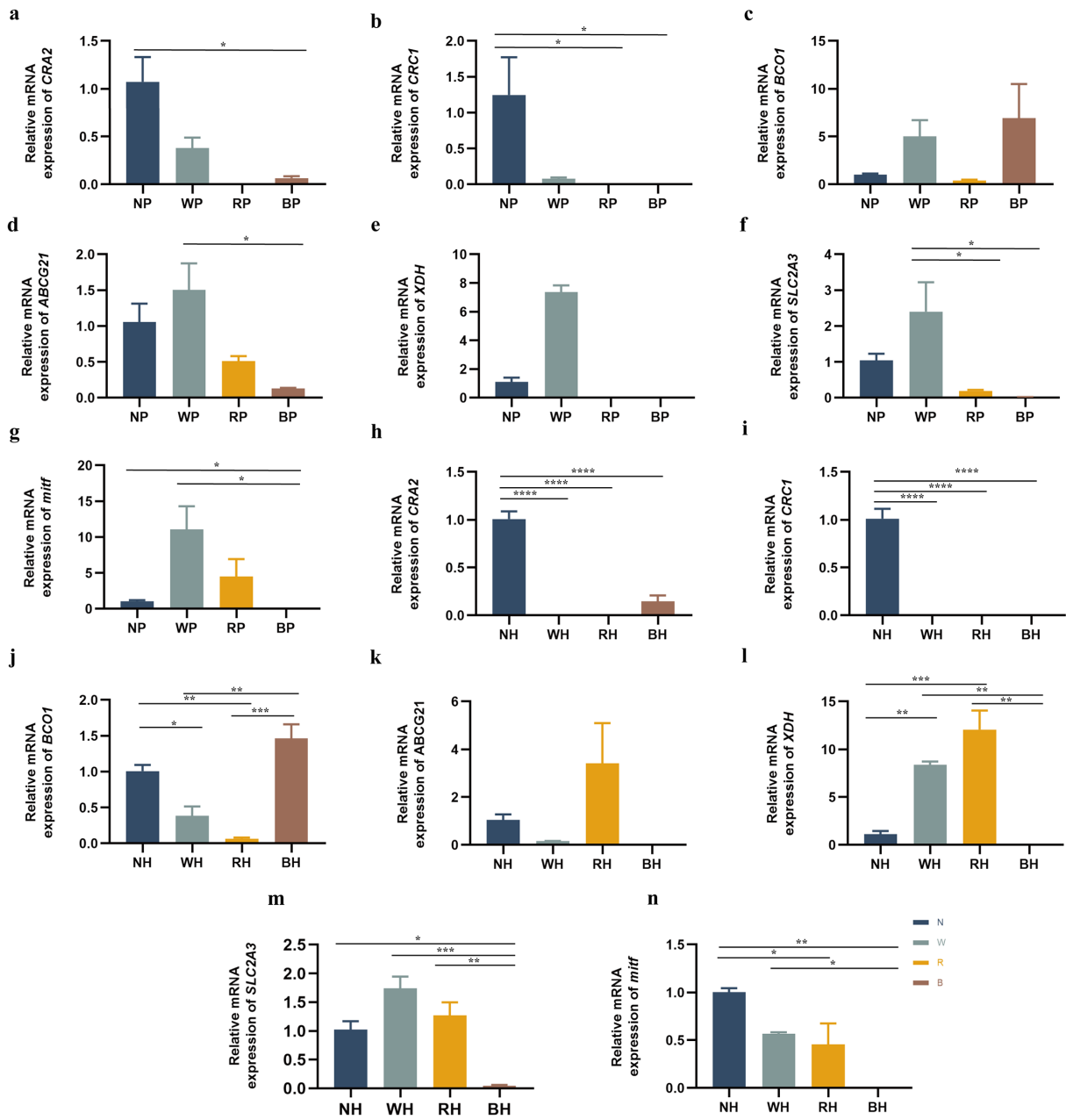
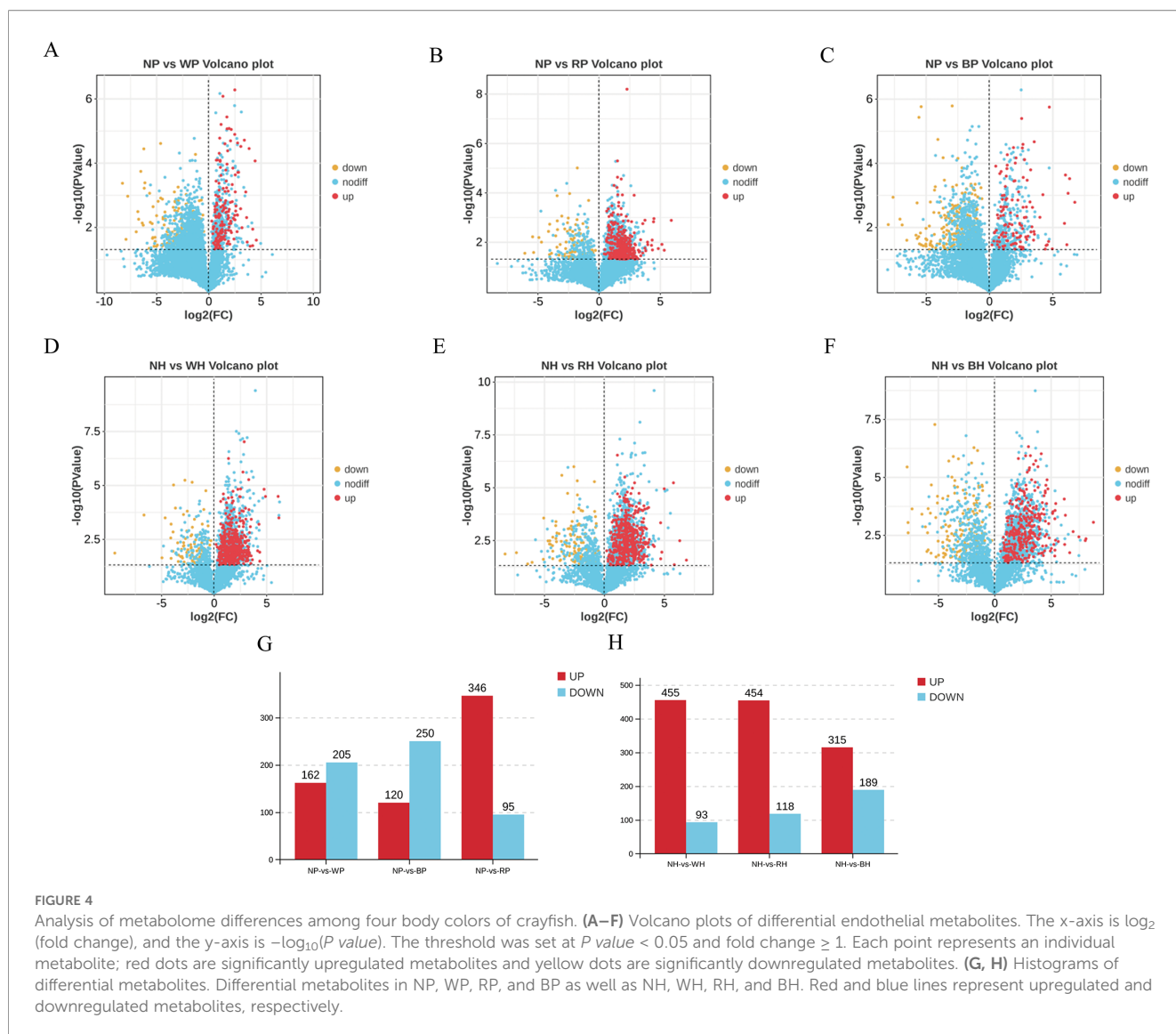


FIGURE 3 (a–g) Expression levels of genes related to body color in endothelia. (NP: normal, endothelium; WP: white crayfish, endothelium; RP: red–orange crayfish, endothelium; BP: blue crayfish endothelium). (h–n) Expression levels of body color–related genes in hepatopancreas. (NH: normal, hepatopancreas; WH: white crayfish, hepatopancreas; RH: red–orange crayfish, hepatopancreas; BH: blue crayfish, hepatopancreas). *, **, ***, and **** denoted that the differences in gene expression in different body colors of crayfish were significant at $P < 0.05$, $P < 0.01$, $P < 0.0001$, and $P < 0.0005$, respectively.

TABLE 2 Number of metabolite identification results.

Tissue	Type	All	Known	Unknown
Endothelium	POS	11611	3049	8562
	NEG	12218	2842	9376
Hepatopancreas	POS	12395	2179	10216
	NEG	11202	1679	9523



coanalyzed pathways in the endothelial comparator group. In addition, 187 differentially expressed genes and 105 differential metabolites were found in the coanalyzed pathways in the hepatopancreatic comparator group. These included genes such as *Scarb1*, *XDH*, and *ABCB* and *ABCG* family members along with differential metabolites such as xanthine, urea, and carotenoid (Supplementary Table 5).

4 Discussion

4.1 Carotenoids and body color

The economic worth of crayfish depends on its color, which is regulated by complex molecular mechanisms and interactions. For instance, carotenoids and pteridine-like pigments in *Neocaridina denticulata sinensis* are associated with red and yellow body coloration in crustaceans (Lin, 2017). In addition, teleost fish body-color studies support this idea (Fang et al., 2022; Johnson and Fuller,

2015). This study detected the type and content of carotenoid in the hepatopancreases and carapaces of the four body colors of crayfish. The carotenoid composition was found to be associated with body color. The carapace and hepatopancreas L^* of white crayfish were significantly higher than those of the normal, red-orange, and blue crayfish. This can be attributed to the presence of the less carotenoid content within the tissues of white crayfish. In a previous study, the carapace and hepatopancreas L^* , a^* , and b^* of *Chinese mitten crabs* were highly correlated with carotenoid content (Li et al., 2021). In the study of body-color regulation in fish and other crustaceans, the body color was determined by the type and content of the carotenoid (Yagiz et al., 2010). In this study, the astaxanthin content of white crayfish carapaces and hepatopancreases was 12.1 and 4.25 times lower than that of the normal crayfish, respectively. This finding is consistent with a previous study on lobsters, in which the pigment content in red lobster is 2.4 times that of the white lobster (Wade et al., 2005).

Combining metabolomics, astaxanthinin, a carotenoid biological metabolic pathway (map00906) of white crayfish

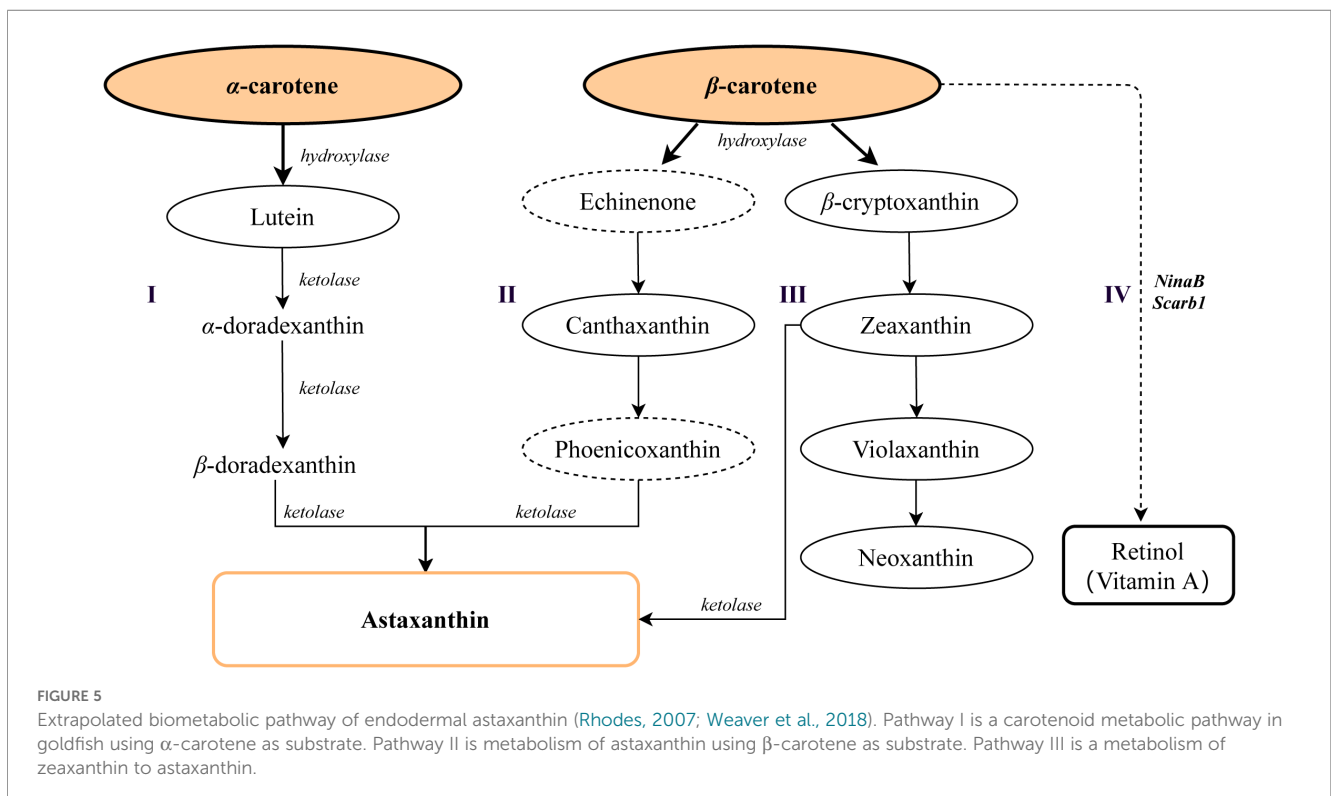
endothelia, was transformed by β -carotene using canthaxanthin. In the study of *Carcinus maenas* carotenoid metabolism, the No.II metabolic pathway in Figure 5 was consistent with the speculation, which was converted from β -carotene to astaxanthin. The type and content of carotenoids in normal-body-color crayfish are greatest in carapace and hepatopancreas, particularly astaxanthin. Combined with the carotenoid synthesis pathways of transcriptome (map00906) and metabolome (map01062) (Figure 5), four astaxanthin synthesis pathways may exist in the endothelia of normal crayfish. The metabolic end products of pathways I, II, III and IV are astaxanthin; therefore, considerable amount of astaxanthin is deposited in the endothelia and hepatopancreas of normal crayfish. For the biological metabolism of ketocarotenoids, β -carotene was used as the substrate, and two hydroxyl and ketone groups were added to each β -ionone ring through a series of reactions. Under the action of hydroxylase and ketolase, it was metabolized to astaxanthin and deposited to the target organ. The difference in the composition and content of carotenoids in the hepatopancreas is likely to be the internal cause of the difference in the shell color phenotype of different strains of crayfish, which aligns with the results of the study of the shell color and embryo of the Chinese mitten crab having green and white shell lines (Zhang et al., 2022, 2023).

4.2 Expression of body color-related genes

BCO1, a crucial gene in carotenoid metabolism, cleaves pertinent carotenoids (Lindqvist and Andersson, 2002; Redmond

et al., 2001; Von Lintig and Vogt, 2000; Wyss et al., 2000). The *BCO* family genes are correlated to the body color of aquatic animals. In our study, NP had the highest concentrations of β -carotene (0.8551 $\mu\text{g}/\text{mL}$); however, BP had a lesser amount (0.2625 $\mu\text{g}/\text{mL}$) than NP. Nevertheless, NP expressed less *BCO1* than BP. WP expressed more *BCO1* expression than NP, although NP had a greater β -carotene concentration. Therefore, we suggest that high *BCO1* expression promotes the conversion of β -carotene into other carotenoids. As shown in Figure 5, β -carotene deposition in the endothelium may be limited, because it could undergo conversion into astaxanthin. Meanwhile, the RP adheres to this pattern. However, all four body colors, endothelium *BCO1* expression was higher than in the hepatopancreas. Consistent with the results of this study, the carotenoid accumulation of the triangle sailing mussel was decreased by the high expression of *HcBCO1* in the triangular pearl mussel (Yan, 2023). Thus, high *BCO1* expression may promote the cleavage of β -cryptoxanthin in the endothelium into other carotenoids. For instance, the expression level of *BCO-like* in the white Patino scallop was significantly higher than in the orange counterparts (Li et al., 2019). *Exopalaemon carinicauda* deepened after knocking out *BCO* (Sun et al., 2020a, b). These observations indicate that *BCO* plays an important role in body-color regulation.

Crustacyanin (*CRCN*) is a protein-binding molecule that binds to ingested astaxanthin, thereby altering the energy level structure of astaxanthin and determining the pattern and color of the carapace (Cianci et al., 2002; Yan, 2023; Zhao et al., 2021). The endothelium and hepatopancreas of crayfish contain two isoforms of the *CRCN* family genes, *CRA2* and *CRC1*. Scholars (Ertl et al., 2013) believed that the expression of the *CRCN-A* and *CRCN-C*



genes of the albino *Metapenaeus penaeus* was significantly lower than that of bright and dark varieties. In this study, these two genes were highly expressed in NP and NH. Moreover, *CRA2* and *CRC1* were expressed in WP, although both at lower levels than in NP. *CRC1* was not expressed in RP, RH, or WH, although it was expressed at low levels in BP and BH. According to research, a lower expression level of the *CRCN* may limit the binding and subsequent utilization of free astaxanthin, which could be one of the reasons why normal crayfish have a dark body color (Jin et al., 2021).

Body-color regulation can be improved by ABCG, a member of the G subfamily of the ABC transporter protein family. The results of this investigation indicate that the expression of *ABCG21* in WP was greater than that in NP, RP, and BP and that the expression of its homologous gene, *ABCG14*, in WP was higher than that of the strains of *Marsupenaeus* species with dark colors (Wang et al., 2023). Notably, the previously mentioned information is consistent with the results of this study. Although most ABC transporter protein family G subfamily members are involved in body-color regulation, their individual methods might differ, necessitating additional research. For instance, a previous study indicates that the *white* gene in *Drosophila* and *Bombyx mori* was homologous to the ABCG homolog in the *Neocaridina denticulata sinensis* body color, and both mutant *Drosophila* bodies containing the *white* gene and *Bombyx mori* eggs were white (Lin, 2017). In the present study, in WP, RP, and WH, the pteridine metabolism related gene *XDH* was strongly expressed; in BP and BH, it was either nonexistent or considerably low. The nontargeted metabolome contained uric acid and xanthine as differentially abundant metabolites. Therefore, we analyzed this possible mechanism of xanthine synthesis of uric acid in white crayfish by combining the expression pattern of *XDH* with untargeted metabolomic results. Our findings are in accordance with a previous study on *Metapenaeus penaeus*, in which the *XDH* gene produced uric acid from xanthine as a defense mechanism against UV damage. When the body is transparent, the expression of *XDH* (Hu et al., 2013), a gene found in the bodies of *Marsupenaeus* species, is high (Lin, 2017).

In crustaceans, body color is regulated in part by genes related to melanin. *mitf* is a crucial regulator of melanocyte formation and plays a role in cell survival, differentiation, and growth. In our study, *mitf* was not expressed in BP but was expressed at high levels in WP, RP, and NP. This finding corresponds to the expression pattern of the *mitfa* gene in all-red Oujiang-colored carp, which have no melanocytes and an all-red phenotype (Yu et al., 2020). The study concluded that although *mitfa* is highly expressed, it does not participate in melanocyte synthesis. In the same way, we only discovered the xanthophores in WP. There were only a few xanthophores found in RP but many erythrophores, many of which covered the NP xanthophores. Melanocytes were absent from WP and RP. *mitf* might promote the xanthophore formation when combined with the discoveries of the study that zebrafish *mitf* is expressed by melanocytes (melanocyte stem cells) and xanthophore precursors (Parichy et al., 2000; Rawls et al.,

2001). Meanwhile, a member of the soluble carrier (SLC) family is *SLC2A3*. Another member, *Slc45a2*, plays a crucial role in melanin deposition in mammals (Graf et al., 2005), and low melanin concentration and misshapen melanocytes are caused by gene mutations in mice and *Oryzias latipes* (Du and Fisher, 2002; Fukamachi et al., 2001). However, SLC family members can also function as carotenoid transporter proteins, particularly for vitamins. Tsukaguchi et al. have identified the *SLC23a1* member as a vitamin C carrier (Tsukaguchi et al., 1999). Investigating the significance of melanin-related genes in the control of body color in crustaceans is vital, because they account for a smaller portion of the body color of crayfish, particularly *mitf*.

4.3 Body color related pathways

In this study, KEGG enrichment analysis was conducted for differentially expressed genes and metabolites in the transcriptome and metabolome. The pathways related to body color regulation that were present in the endothelial and hepatopancreatic comparative groups were vitamin digestion and absorption, retinol digestion and absorption, and purine metabolism. Pigments in crustaceans not only regulate body color but also maintain balanced physiological metabolic functions, such as oxidative metabolism, visual maintenance, and defense mechanisms.

In this study, Scavenger receptor class B type I (*Scarb1*) of vitamin digestion and absorption was significantly upregulated in NP vs. RP. However, there were no significant differences in the expression in hepatopancreas. Because *Scarb1* is an HDL receptor (high-density lipoprotein) that binds to cholesterol transport particles and promotes cellular uptake of carotenoids, it is highly focused on by scholars (Toomey et al., 2017). A study by Kanika et al. found that *Scarb1* expression in the skin of white mutant Oujiang carp was lower than that in wild red and mutant red Oujiang carp (Kanika et al., 2023). Tian et al. have shown that the use of miR-430b to limit *Scarb1* expression disturbs carotenoid metabolism and decreases chromatophore distribution density, thereby weakening the skin redness value of koi carp (Tian et al., 2022). This study found that *Scarb1* expression in white crayfish (WP) is higher than in normal crayfish (NP) possibly owing to the low carotenoid content, resulting in decreased oxidation capacity. *Scarb1* is used to maintain antioxidant capacity by converting β -carotene to retinol.

The retinol metabolism pathway plays an important role in the growth, development, and body-color regulation of aquatic animals (Bi et al., 2024; Wiseman et al., 2017). Retinol is a form of vitamin A, which can be transformed through metabolic pathways in organisms into active forms such as retinol ester and retinol acid. It is involved in regulating the growth, differentiation, antioxidant and immune functions, reproduction and embryonic development of almost all cells (Das et al., 2014). Retinol deficiency can cause visual system disorders (Saleh et al., 1995) such as, exophthalmos (Yang et al., 2008), small eyes or retinopathy, and retinal

development disorders. After adding an appropriate amount of retinol to the shrimp feed, the vision became sensitive, the function became normal, and the eye tissue is not distorted (Chen and Li, 1994). Carotenoid metabolism indirectly promotes retinol metabolism in the digestive system, of which β -carotene is metabolized into retinol via the regulation of *Scarb1*, which participates in pigmentation, antioxidation, and development. In this study, *Scarb1* expression in the hepatopancreas of normal crayfish was upregulated and promoted pigmentation. In the study of crap, when *Scarb1* was knocked out, the red skin turned white, and the type and content of astaxanthin decreased. *Scarb1* converts the part of β -carotene to retinol (vitamin A) to maintain a balanced physiological function in the body. White crayfish use retinol to compensate for the deficiencies in antioxidant capacity, reproductive capacity and visual system.

The purine metabolic pathway is an important in regulating the balance of ammonia nitrogen in insects and crustaceans. Crustaceans use xanthine as a substrate to decompose urea into ammonia and CO_2 under the action of urease. Because ammonia has certain toxicity in animals, it must be promptly removed (Liu et al., 2005). In the metabolic process of silkworm pigment, *XDH* oxidizes xanthine to urate, and the accumulation of urate increases the transparency of the body and strengthens its defenses against ultraviolet light (Hu et al., 2013). *XDH* is highly expressed in the stomach and heart of Pacific shrimp (*Marsupenaeus japonicus*), which helps to scavenge free radicals and resist *Vibrio*, and controls the occurrence of white spot syndrome (Lin, 2017; Okamura et al., 2018). In this study, *XDH* was significantly upregulated in WP, and uric acid was downregulated, xanthine and uric acid accumulation increased. The body transparency of white crayfish was increased, which could strengthen their defense mechanism against ultraviolet light.

5 Conclusion

The various colors of crayfish are an excellent subject for studying crustacean body colors. In this study, we discovered that crayfish with white bodies contained only xanthophores, whereas crayfish with red-orange, blue, and normal colors predominantly contained erythrophores. Crayfish normal body color have highest abundance of carotenoids. Conversely, white crayfish exhibited the lowest carotenoid content and diversity. A consistent pattern of variation in the apparent body color L^* , a^* , and b^* was observed between the hepatopancreases and carapaces of the crayfish. By jointly analyzing the metabolic pathways of carotenoids in the transcriptome and metabolome, this study identified four carotenoid metabolic pathways. In the digestion and absorption pathways of retinol and vitamins in white crayfish, a lack of retinol compensatory carotenoids was observed, leading to oxidation deficiency. This deficiency, in turn, can prevent pigments from effectively regulating body color. This investigation can help identify carotenoid-related metabolic routes in crustaceans and

establish a foundation for future gene-editing techniques to regulate crustacean body color.

Data availability statement

The datasets presented in this study can be found in online repositories. The names of the repository/repositories and accession number(s) can be found in the article/Supplementary Material.

Ethics statement

The animal studies were approved by Institution Animal Care and Use Committee of Shanxi Agricultural University. The studies were conducted in accordance with the local legislation and institutional requirements. Written informed consent was obtained from the owners for the participation of their animals in this study.

Author contributions

QL: Visualization, Funding acquisition, Data curation, Resources, Writing – review & editing, Conceptualization, Writing – original draft. ZH: Methodology, Formal analysis, Supervision, Software, Writing – original draft, Resources, Investigation, Visualization. LY: Validation, Formal analysis, Data curation, Writing – original draft, Resources, Supervision. XL: Resources, Methodology, Writing – review & editing. HZ: Supervision, Writing – review & editing, Validation. LZ: Conceptualization, Software, Writing – review & editing, Investigation, Project administration, Formal analysis. GG: Data curation, Project administration, Resources, Writing – original draft. YL: Visualization, Supervision, Writing – review & editing, Formal analysis. LX: Writing – review & editing, Supervision, Validation, Data curation. JS: Methodology, Writing – review & editing, Resources, Investigation. SL: Resources, Writing – review & editing, Formal analysis, Software. WW: Visualization, Validation, Writing – review & editing. XW: Project administration, Methodology, Writing – review & editing, Resources.

Funding

The author(s) declared that financial support was received for this work and/or its publication. The Biological Breeding Project of Shanxi Agricultural University (YZGC133), the “1331 Project” Key Discipline of Animal Science of Shanxi Province (J201911306), the Earmarked Fund for Modern Agro-industry Technology Research System of Shanxi Province (2022QT024, 2023QT123), Shanxi Agricultural University’s “Introduction of talent research start-up project” (2023BQ08), International Science and Technology Cooperation Programme of the Ministry of Science and

Technology of China (2019YFE0116800, SQ2023YFE0102235), National Natural Science Foundation of China (32303039), Shanxi doctoral graduates to work in Shanxi reward funds scientific research project (SXBYKY2023032).

Conflict of interest

The authors declared that this work was conducted in the absence of any commercial or financial relationships that could be construed as a potential conflict of interest.

Generative AI statement

The author(s) declared that Generative AI was not used in the creation of this manuscript.

Any alternative text (alt text) provided alongside figures in this article has been generated by Frontiers with the support of artificial

intelligence and reasonable efforts have been made to ensure accuracy, including review by the authors wherever possible. If you identify any issues, please contact us.

Publisher's note

All claims expressed in this article are solely those of the authors and do not necessarily represent those of their affiliated organizations, or those of the publisher, the editors and the reviewers. Any product that may be evaluated in this article, or claim that may be made by its manufacturer, is not guaranteed or endorsed by the publisher.

Supplementary material

The Supplementary Material for this article can be found online at: <https://www.frontiersin.org/articles/10.3389/fmars.2025.1731102/full#supplementary-material>

References

- Babin, A., Moreau, J., and Moret, Y. (2019). Storage of carotenoids in crustaceans as an adaptation to modulate immunopathology and optimize immunological and life-history strategies. *BioEssays* 41, 1800254.
- Babin, A., Motreuil, S., Teixeira, M., Bauer, A., Rigaud, T., Moreau, J., et al. (2020). Origin of the natural variation in the storage of dietary carotenoids in freshwater amphipod crustaceans. *PLoS One* 15(4), e0231247.
- Bi, J. L., Lin, C., Meng, Z. Y., Zhou, J., Yaguo, X., and Peng, X. (2024). Integrative transcriptomics and metabolomics analysis of body color formation in the common carp. *Aquaculture* 579, 740143. doi: 10.1016/j.aquaculture.2023.740143
- Bonafé, L., Thöny, B., Penzien, J. M., Czarnecki, B., and Blau, N. (2001). Mutations in the sepiapterin reductase gene cause a novel tetrahydrobiopterin-dependent monoamine-neurotransmitter deficiency without hyperphenylalaninemia. *Am. J. Hum. Genet.* 69, 269–277.
- Caro, T. (2005). The Adaptive Significance of Coloration in Mammals. *BioScience* 55, 125–136. doi: 10.1641/0006-3568(2005)055[0125:TASOCI]2.0.CO;2
- Chen, S. Q., and Li, A. J. (1994). Investigation on nutrition of vitamin A for shrimp *Penaeus chinensis*: I. Effects of vitamin on shrimp's growth and visual organ. *Acta Zoologica Sin.* 40, 266–273+339.
- Chen, S. F., Zhou, Y. Q., Chen, Y. R., and Gu, J. (2018). fastp: an ultra-fast all-in-one FASTQ preprocessor. *Bioinformatics* 34, i884–i890. doi: 10.1093/bioinformatics/bty560
- Cianci, M., Rizkallah, P. J., Olczak, A., Raftery, J., Chayen, N. E., Zagalsky, P. F., et al. (2002). The molecular basis of the coloration mechanism in lobster shell: β -Crustacyanin at 3.2-Å resolution. *Proc. Natl. Acad. Sci.* 99, 9795–9800. doi: 10.1073/pnas.152088999
- Danecek, P., Bonfield, J. K., Liddle, J., Marshall, J., Ohan, V., Pollard, M. O., et al. (2021). Twelve years of SAMtools and BCFtools. *Gigascience* 10, giab008. doi: 10.1093/gigascience/giab008
- Das, B. C., Thapa, P., Karki, R., Das, S., Mahapatra, S., Liu, T.-C., et al. (2014). Retinoic acid signaling pathways in development and diseases. *Bioorganic Medicinal Chem.* 22, 673–683.
- Ding, J. Y., and Kangqin, X. J. (2010). Analysis and Evaluation of Muscle Nutritional Components of crayfish, *Procambarus clarkii*. *Fisheries Sci. & Technology Inf.* 6, 298–301. doi: 10.3969/j.issn.1001-1994.2010.06.009
- Du, J. Y., and Fisher, D. E. (2002). Identification of aim-1 as the under white mouse mutant and its transcriptional regulation by MITF. *J. Biol. Chem.* 277, 402–406. doi: 10.1074/jbc.m110229200
- Ertl, N. G., Elizur, A., Brooks, P., Kuballa, A. V., Anderson, T. A., and Knibb, W. R. (2013). Molecular characterisation of colour formation in the prawn *Fenneropenaeus merguensis*. *PLoS One* 8, e56920. doi: 10.1371/journal.pone.0056920
- Fang, W. Y., Huang, J. R., Li, S. Z., and Lu, J. G. (2022). Identification of pigment genes (melanin, carotenoid and pteridine) associated with skin color variant in red tilapia using transcriptome analysis. *Aquaculture* 547, 737429. doi: 10.1016/j.aquaculture.2021.737429
- Fukamachi, S., Shimada, A., and Shima, A. (2001). Mutations in the gene encoding B, a novel transporter protein, reduce melanin content in medaka. *Nat. Genet.* 28, 381–385. doi: 10.1038/ng584
- Graf, J., Hodgson, R., and Van Daal, A. (2005). Single nucleotide polymorphisms in the MATP gene are associated with normal human pigmentation variation. *Hum. Mutat.* 25, 278–284. doi: 10.1002/humu.20143
- Haas, B. J., Papanicolaou, A., Yassour, M., Grabherr, M., Blood, P. D., Bowden, J., et al. (2013). De novo transcript sequence reconstruction from RNA-seq using the Trinity platform for reference generation and analysis. *Nat. Protoc.* 8, 1494–1512. doi: 10.1038/nprot.2013.084
- Hu, J., Feng, C., Ma, X., Wu, L. M., Liu, H. F., Song, H. M., et al. (2020). Molecular cloning and expression of sepiapterin reductase in Japanese ornamental carp (*Cyprinus carpio* var. *koi*). *J. Fisheries China* 44, 551–561. doi: 10.11964/jfc.20190711869
- Hu, Y. G., Shen, Y. H., Zhang, Z., and Shi, G. Q. (2013). Melanin and urate act to prevent ultraviolet damage in the integument of the silkworm, *Bombyx mori*. *Arch. Insect Biochem. Physiol.* 83, 41–55. doi: 10.1002/arch.21096
- Ichikawa, Y., Ohtani, H., and Miura, I. (1998). The erythrophore in the larval and adult dorsal skin of the brown frog, *Rana ornativentris*: its differentiation, migration, and pigmentary organelle formation. *Pigment Cell Res.* 11, 345–354. doi: 10.1111/j.1600-0749.1998.tb00493.x
- Jiao, Y. L., Chen, H. C., Huang, X. X., and Wang, W. L. (2023). Comparison of Carotenoid Content in Brine Shrimp *Artemia* Decapsulated Cysts and Nauplius From Three Locations. *Chin. J. Fisheries* 36, 69–74+8.
- Jin, Y., Li, S. H., Yu, Y., Zhang, C. S., Zhang, X. J., and Li, F. H. (2021). Transcriptome analysis provides insights into the mechanism of astaxanthin enrichment in a mutant of the ridgetail white prawn *Exopalaemon carinicauda*. *Genes* 12, 618. doi: 10.3390/genes12050618
- Johnson, A. M., and Fuller, R. C. (2015). The meaning of melanin, carotenoid, and pterin pigments in the bluefin killifish, *Lucania goodei*. *Behav. Ecol.* 26, 158–167. doi: 10.1093/beheco/aru164
- Kanika, N. H., Ke, J., Mandal, R. N., Wang, J., and Wang, C. H. (2023). Comparative transcriptome and metabolome analyses of wild and mutant Oujiang color common carp through editing SCARB1 gene by CRISPR/Cas technology. *Aquaculture* 577, 739901. doi: 10.1016/j.aquaculture.2023.739901
- Kim, D., Langmead, B., and Salzberg, S. L. (2015). HISAT: a fast spliced aligner with low memory requirements. *Nat. Methods* 12, 357–360. doi: 10.1038/nmeth.3317
- Kimura, T. (2021). Pigments in Teleosts and their Biosynthesis. *Pigments Pigment Cells Pigment Patterns*, 127–148. doi: 10.1007/978-981-16-1490-3
- Li, Q. Q., Sun, Q. F., Liu, Q., Cheng, Y. X., and Wu, X. G. (2021). Estimation of genetic parameters for carotenoid traits in Chinese mitten crab, *Eriocheir sinensis*, females. *Aquaculture* 532, 735990. doi: 10.1016/j.aquaculture.2020.735990

- Li, X., Wang, S. Y., Xun, X. G., Zhang, M. R., Wang, S., Li, H. D., et al. (2019)1864). A carotenoid oxygenase is responsible for muscle coloration in scallop. *Biochim. Biophys. Acta (BBA)-Molecular Cell Biol. Lipids* 7, 966–975. doi: 10.1016/j.bbalip.2019.03.003
- Lin, S. (2017). *Searching and Identifying Pigmentation Genes from Neocaridina denticulata sinensis* (Postgraduate, Jimei University).
- Lindqvist, A., and Andersson, S. (2002). Biochemical properties of purified recombinant human β -carotene 15, 15'-monooxygenase. *J. Biol. Chem.* 277, 23942–23948. doi: 10.1041/0006-3568(2005)055[0125:TASOCI]2.0.CO;2
- Liu, J., Dai, F. Y., Zhu, Y., and Lu, C. (2005). Purine metabolism in silkworm mutants. *Newslett. Sericultural Sci.* 25, 9–14.
- Liu, S. K., Li, Q., and Liu, Z. J. (2013). Genome-wide identification, characterization and phylogenetic analysis of 50 catfish ATP-binding cassette (ABC) transporter genes. *PLoS One* 8, e63895. doi: 10.1371/journal.pone.0063895
- Liu, S. M., Zhou, S., Tian, L., Guo, E. E., Luan, Y. X., Zhang, J. Z., et al. (2011). Genome-wide identification and characterization of ATP-binding cassette transporters in the silkworm, *Bombyx mori*. *BMC Genomics* 12, 1–15.
- Love, M. I., Huber, W., and Anders, S. (2014). Moderated estimation of fold change and dispersion for RNA-seq data with DESeq2. *Genome Biol.* 15, 1–21. doi: 10.1186/s13059-014-0550-8
- Nakatani, I. (1999). An albino of the crayfish *Procambarus clarkii* (Decapoda: Cambaridae) and its offspring. *J. Crustacean Biol.* 19, 380–383. doi: 10.1163/193724099X00196
- Okamura, Y., Inada, M., Elshopey, G. E., and Itami, T. (2018). Characterization of xanthine dehydrogenase and aldehyde oxidase of *Marsupenaeus japonicus* and their response to microbial pathogen. *Mol. Biol. Rep.* 45, 419–432.
- Oliphant, L. W., and Hudon, J. (1993). Pteridines as reflecting pigments and components of reflecting organelles in vertebrates. *Pigment Cell Res.* 6, 205–208. doi: 10.1111/j.1600-0749.1993.tb00603.x
- Parichy, D. M., Ransom, D. G., Paw, B., Zon, L. I., and Johnson, S. L. (2000). An orthologue of the kit-related gene *fms* is required for development of neural crest-derived xanthophores and a subpopulation of adult melanocytes in the zebrafish, *Danio rerio*. *Development* 127, 3031–3044. doi: 10.1242/dev.127.14.3031
- Rawls, J. F., Mellgren, E. M., and Johnson, S. L. (2001). How the zebrafish gets its stripes. *Dev. Biol.* 240, 301–314. doi: 10.1006/dbio.2001.0418
- Redmond, T. M., Gentleman, S., Duncan, T., Yu, S., Wiggert, B., Gantt, E., et al. (2001). Identification, expression, and substrate specificity of a mammalian β -carotene 15, 15'-dioxygenase. *J. Biol. Chem.* 276, 6560–6565. doi: 10.1074/jbc.M009030200
- Rhodes, A. C. (2007). *Dietary effects on carotenoid composition in the marine harpacticoid copepod Nitokra lacustris* Vol. 29p (Oxford University Press), i73–i83.
- Saccetti, E., Hoefsloot, H. C., Smilde, A. K., Westerhuis, J. A., and Hendriks, M. M. (2014). Reflections on univariate and multivariate analysis of metabolomics data. *Metabolomics* 10, 361–374. doi: 10.1007/s11306-013-0598-6
- Saleh, G., Eleraky, W., and Gropp, J. M. (1995). A short note on the effects of vitamin A hypervitaminosis and hypovitaminosis on health and growth of *Tilapia nilotica* (*Oreochromis niloticus*). *J. Appl. Ichthyology* 11, 382–385.
- Saunders, L. M., Mishra, A. K., Aman, A. J., Lewis, V. M., Toomey, M. B., Packer, J. S., et al. (2019). Thyroid hormone regulates distinct paths to maturation in pigment cell lineages. *eLife* 8, e45181. doi: 10.7554/eLife.45181
- Shimaya, M., et al. (1972). The Biosynthesis of Astaxanthin—VIII: The Conversion of Labeled β -carotene-15, 15'-3 h₂ into Astaxanthin in Prawn, *Penaeus japonicus* Bate. *Nippon suisan gakkaiishi* 38, 1171. doi: 10.2331/suisan.38.1171
- Simpson, K., and Chichester, C. (1976). The biosynthesis of astaxanthin. XVIII. The metabolism of the carotenoids in the prawn, *Penaeus japonicus* Bate. *Japanese Soc. Fisheries Sci.* 42, 197–202. doi: 10.2331/suisan.42.197
- Strychalski, J., Gugolek, A., Antoszkiewicz, Z., Fopp-Bayat, D., Kaczorek-Lukowska, E., Snarska, A., et al. (2022). The effect of the BCO2 genotype on the expression of genes related to carotenoid, retinol, and α -tocopherol metabolism in rabbits fed a diet with aztec marigold flower extract. *Int. J. Mol. Sci.* 23, 10552. doi: 10.3390/ijms231810552
- Stuart-Fox, D., and Moussalli, A. (2009). Camouflage, communication and thermoregulation: lessons from colour changing organisms. *Philos. T R Soc. B.* doi: 10.1098/rstb.2008.0254
- Sun, Y. Y., Liu, M. F., Yan, C. C., Yang, H., Wu, Z. X., Liu, Y. J., et al. (2020a). CRISPR/Cas9-mediated deletion of β , β -carotene 9', 10'-oxygenase gene (EcbCO2) from *Exopalaemon carinicauda*. *Int. J. Biol. Macromolecules* 151, 168–177. doi: 10.1016/j.ijbiomac.2020.02.073
- Sun, Y. Y., Yan, C. C., Liu, M. F., Liu, Y. J., Wang, W. Z., Cheng, W., et al. (2020b). CRISPR/Cas9-mediated deletion of one carotenoid isomeroxygenase gene (EcninaB-X1) from *Exopalaemon carinicauda*. *Fish Shellfish Immunol.* 97, 421–431. doi: 10.1016/j.fsi.2019.12.037
- Tian, X., Peng, N. N., Ma, X., Wu, L. M., Shi, X., Liu, H. F., et al. (2022). microRNA-430b targets scavenger receptor class B member 1 (scarb1) and inhibits coloration and carotenoid synthesis in koi carp (*Cyprinus carpio* L.). *Aquaculture* 546, 737334. doi: 10.1016/j.aquaculture.2021.737334
- Toomey, M. B., Lopes, R. J., Araújo, P. M., Johnson, J. D., Gazda, M. A., Afonso, S., et al. (2017). High-density lipoprotein receptor SCARB1 is required for carotenoid coloration in birds. *Proc. Natl. Acad. Sci.* 114, 5219–5224. doi: 10.1073/pnas.1700751114
- Tsukaguchi, H., Tokui, T., Mackenzie, B., Berger, U. V., Chen, X. Z., Wang, Y. X., et al. (1999). A family of mammalian Na⁺-dependent L-ascorbic acid transporters. *Nature* 399, 70–75. doi: 10.1038/19986
- Volkening, A., and Sandstede, B. (2018). Iridophores as a source of robustness in zebrafish stripes and variability in *Danio* patterns. *Nat. Commun.* 9, 3231. doi: 10.1038/s41467-018-05629-z
- Von Lintig, J., and Vogt, K. (2000). Filling the gap in vitamin A research: molecular identification of an enzyme cleaving β -carotene to retinal. *J. Biol. Chem.* 275, 11915–11920. doi: 10.1074/jbc.275.16.11915
- Wade, N. M., Anderson, M., Sellars, M. J., Tume, R. K., Preston, N. P., and Glencross, B. D. (2012). Mechanisms of colour adaptation in the prawn *Penaeus monodon*. *J. Exp. Biol.* 215, 343–350. doi: 10.1242/jeb.064592
- Wade, N. M., Gabaudan, J., and Glencross, B. D. (2017). A review of carotenoid utilisation and function in crustacean aquaculture. *Rev. Aquaculture* 9, 141–156. doi: 10.1111/raq.12109
- Wade, N., Goulter, K. C., Wilson, K. J., Hall, M. R., and Degnan, B. M. (2005). Esterified astaxanthin levels in lobster epithelia correlate with shell colour intensity: potential role in crustacean shell colour formation. *Comp. Biochem. Physiol. Part B: Biochem. Mol. Biol.* 141, 307–313.
- Wang, M. R. (2012) in *Functional Characteration of one prawn lipocalin gene (Macrobrachium rosenbergii)* (Doctor, Zhejiang University).
- Wang, P. P., Xie, S. M., Li, X. Y., Zhu, J. W., You, Z. Q., Zhou, X. L., et al. (2023). Transcriptome analysis provides insights into the mechanism of carapace stripe formation in two closely related *Marsupenaeus* species. *Front. Mar. Sci.* doi: 10.3389/fmars.2023.1234940
- Warnes, G., Bolker, B., Lumley, T., and Johnson, R. (2018). *gmodels: Various R programming tools for model fitting (version 2.18. 1)*.
- Weaver, R. J., Cobine, P. A., and Hill, G. E. (2018). On the bioconversion of dietary carotenoids to astaxanthin in the marine copepod, *Tigriopus californicus*. *J. Plankton Res.* 40, 142–150. doi: 10.1093/plankt/fbx072
- Wijnen, B., Leertouwer, H. L., and Stavenga, D. G. (2007). Colors and pterin pigmentation of pierid butterfly wings. *J. Insect Physiol.* 53, 1206–1217. doi: 10.1016/j.jinsphys.2007.06.016
- Wiseman, E. M., Bar-El Dadon, S., and Reifen, R. (2017). The vicious cycle of vitamin A deficiency: A review. *Crit. Rev. Food Sci. Nutr.* 57, 3703–3714. doi: 10.1080/10408398.2016.1160362
- Wu, T. Z., Hu, E. Q., Xu, S. B., Chen, M. J., Guo, P. F., Dai, Z. H., et al. (2021). clusterProfiler 4.0: A universal enrichment tool for interpreting omics data. *Innovation* 2, (3). doi: 10.1016/j.xinn.2021.100141
- Wyss, A., Wirtz, G., Woggon, W. D., Brugger, R., Wyss, M., Friedlein, A., et al. (2000). Cloning and Expression of β , β -Carotene 15, 15'-Dioxygenase. *Biochem. Biophys. Res. Commun.* 271, 334–336. doi: 10.1006/bbrc.2000.2619
- Xiao, Q., Zhang, M. T., Wu, Y., Ding, H., Lei, J. C., Zhu, S. L., et al. (2020). Prediction of potential distribution of the invasive species *Procambarus clarkii* in China based on ecological niche models. *Chin. J. Appl. Ecol.* 31, (1). doi: 10.13287/j.1001-9332.202001.029
- Yagiz, Y., Kristinsson, H. G., Balaban, M. O., Welt, B. A., Raghavan, S., and Marshall, M. R. (2010). Correlation between astaxanthin amount and a* value in fresh Atlantic salmon (*Salmo salar*) muscle during different irradiation doses. *Food Chem.* 120, 121–127. doi: 10.1016/j.foodchem.2009.09.086
- Yan, L. (2023). Identification and functional study of carotenoid metabolizing genes GSTP1, BCO1 and BCO2 in *Hyriopsis cumingii*. *Postgraduate*.
- Yang, Q. H., Zhou, X. Q., Jiang, J., and Liu, Y. (2008). Effect of dietary vitamin A deficiency on growth performance, feed utilization and immune responses of juvenile Jian carp (*Cyprinus carpio* var. *Jian*). *Aquaculture Res.* 39, 902–906.
- Yu, L. W., Cao, S. Y., Wang, J., and Wang, C. H. (2020). Formation of melanin and mitfa *in-situ* in the Oujiang color common carp (*Cyprinus carpio* var. *color*). *J. Shanghai Ocean Univ.* 29, 481–488. doi: 10.12024/j.sou.20190502668
- Yu, Y. Y., Wang, D., Xu, J., Xu, B., Ma, B. S., and Zhu, X. Y. (2022). Transcriptome analysis of the hepatopancreas of *Procambarus clarkii* under hypoxic stress. *Journal* 52, 26–35. doi: 10.13721/j.cnki.dsyy.2022.06.010
- Zhang, D. D., Fan, C. W., Jiang, X. D., Cheng, Y., and Wu, X. G. (2022). Comparison of reproductive performance, embryo color and biochemical composition of white and green carapace strains of Chinese mitten crab (*Eriocheir sinensis*). *South China Fisheries Sci.* 18, 102–110. doi: 10.12131/2021026
- Zhang, D. D., Fan, C. W., Jiang, X. D., Cheng, Y. X., and Wu, X. G. (2023). Comparison of edible yield, carotenoid content and nutritional composition between the white carapace strain and green carapace strain of adult *Eriocheir sinensis*. *J. Fisheries China* 47, 122–134. doi: 10.11964/jfc.20210612886
- Zhao, C., Peng, C., Fan, S. G., Wang, P. F., Yan, L. L., Xie, Z. F., et al. (2021). Identification of a novel crustacyanin-like lipocalin in *Penaeus monodon*: molecular cloning, tissue distribution and its functional studies in astaxanthin accumulation. *Aquaculture* 539, 736615. doi: 10.1016/j.aquaculture.2021.736615